Z. Phys. Chem. **225** (2011) 1457–1469 / **DOI** 10.1524/zpch.2011.0197

Dispersed Fluorescence Spectra of 1H- and 1D-Indazole

By Hauke Nicken[1], Friedrich Temps[1,*], and Erko Jalviste[2]

[1] Institut für Physikalische Chemie, Christian-Albrechts-Universität zu Kiel, Olshausenstr. 40, 24098 Kiel, Germany
[2] Institute of Physics, University of Tartu, Riia 142, 51014 Tartu, Estonia

Dedicated to Katharina Kohse-Höinghaus on the occasion of her 60th birthday

(Received October 17, 2011; accepted in revised form November 14, 2011)

Laser Induced Fluorescence / Dispersed Fluorescence / Molecular Beams / Normal Modes / Indazole

Dispersed fluorescence (DF) spectra of jet-cooled indazole (Ia-*h*) and its singly-deuterated isotopologue (Ia-*d*) were recorded following excitation of the origin band of the $S_1(^1A') \leftarrow S_0(^1A')$ electronic transition. The spectra were analyzed and assigned with the help of vibrational frequency calculations by density functional theory (DFT) at the TPSS/aug-cc-pVTZ level. The calculated and measured S_0 state vibrations are in agreement within $\leq 3\%$. The obtained results for the two Ia monomers form the basis for an analysis of the electronic spectra of the hydrogen-bonded dimers Ia_2-*hh*, Ia_2-*dd* and Ia_2-*hd* and a determination of the exciton splitting in the dimer in a forthcoming paper.

1. Introduction

Indazole (Ia) is a planar aza-aromatic bicyclic compound that can exist in two tautomeric forms differing only in the position of the imino group as sketched in Fig. 1. Quantum chemical calculations [1,2] showed that the 1H tautomer (Fig. 1a) is more stable by ≈ 15 kJ/mol than the 2H tautomer (Fig. 1b), consistent with the predominance of 1H-indazole under normal room temperature conditions and in molecular beam experiments.

Indazole molecules have been the subject of a variety of investigations, among them theoretical studies and several measurements by microwave, infrared, and ultraviolet/visible spectroscopy [1–12]. The $S_1(A') \leftrightarrow S_0(A')$ electronic transition of 1H-indazole (Ia-*h*) around $\lambda \approx 290$ nm that is of interest here has a strong origin band at $\nu_0 = 34471.69\ \mathrm{cm}^{-1}$ and well structured vibrational progressions [9,10]. In an earlier publication, we investigated the $S_1 \leftrightarrow S_0$ transition of jet-cooled Ia-*h* by laser-induced

* Corresponding author. E-mail: temps@phc.uni-kiel.de

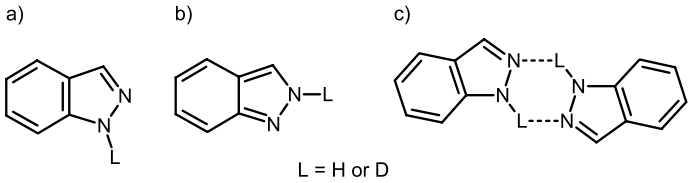

Fig. 1. Structures of **(a)** 1H/1D-indazole (Ia-*h*, Ia-*d*), **(b)** 2H/2D-indazole (Ia-*h′*, Ia-*d′*), and **(c)** the three H-bonded dimers of 1H- and 1D-indazole (Ia_2-*hh*, Ia_2-*hd*, Ia_2-*dd*). L = H or D indicates a hydrogen or a deuterium atom.

fluorescence (LIF) excitation and dispersed fluorescence (DF) spectroscopy [10]. DF spectra were recorded after excitation of several vibronic bands up to 1270 cm^{-1} above the electronic origin. The vibrational modes in the ground and excited state were assigned based on the measured band frequencies and intensities, MP2/6-31G frequency calculations, and available infrared absorption data. The results provided detailed information on the correspondence between ground- and excited-state normal modes.

This paper gives an analogous account on the singly-deuterated isotopologue 1D-indazole (Ia-*d*). It confines itself to an analysis of the DF spectrum from the S_1 origin of Ia-*d*. The improved accuracy of quantum chemical frequency calculations today compared to the earlier work [10] allowed us to not only identify most of the S_0 vibrations of Ia-*d* in the DF spectrum from its $S_1 \leftarrow S_0$ origin band, but also to reanalyze the DF spectra of Ia-*h*. The comparison of the spectra of Ia-*d* and Ia-*h* confirms the vibrational assignments, because most of the observed bands are affected little by the deuteration as long as the ND group does not contribute much to the vibrations.

The need for accurate data on the ground-state vibrations of Ia-*h* and Ia-*d* stems from our forthcoming investigation of the hydrogen-bonded dimers (see Fig. 1c) of both indazole isotopologues [13]. Having a hydrogen donating and a hydrogen accepting site in the five-membered pyrazole ring side-by-side, indazole is known to form H-bridged self-complexes under supersonic jet expansion conditions [14]. The observed structures are similar to those of pyrazole, which likes to form cyclic dimers, trimers and tetramers in the solid state [15,16], trimers in liquid solution [17], and dimers, trimers and even larger aggregates in the gas phase [18–20]. However, pyrazole and its complexes cannot be easily studied using nanosecond laser-induced fluorescence excitation or dispersed fluorescence spectroscopy, because its UV absorption spectrum is broad and diffuse without any resolved vibrational structure [21] due to the rapid N–H bond fission after $\pi\pi^*$ excitation *via* the $\pi\sigma^*$ state [22]. In contrast, fluorescence is the method of choice for indazole [10,14]. The dominating structure among the indazole complexes in a molecular beam is the symmetric dimer, in which the monomer moieties are linked by two H-bonds as depicted in Fig. 1c [14]. Test measurements of DF spectra of jet-cooled dimer isotopologues indicated that, in contrast to the intermolecular modes, the intramolecular vibrations in the dimers and parent monomers can be directly related. Being ideal model systems for doubly H-bonded molecular complexes, a detailed analysis of the vibronic spectra of the homo- and hetero-dimers Ia_2-*hh*, Ia_2-*dd*, and Ia_2-*hd* (Fig. 1c) provides novel insight not only into the respective intermolecular vibrations in the complexes, but also allows us to determine the size of the elusive exciton splitting energy in the dimer [13].

2. Experimental and computational methods

The experiments employed a similar setup as before [10,14]. A pulsed supersonic jet containing indazole in helium carrier gas at a backing pressure of ≈ 4 bar was formed by a heated pulsed valve (General Valve) with a 0.8 mm pinhole. The solid indazole sample was kept in a reservoir at $\approx 140\,^{\circ}\mathrm{C}$ attached directly to the valve. A partially deuterated sample was prepared before by dissolving a few grams of normal indazole (Sigma-Aldrich, 98%) in excess D_2O with a small amount of CD_3OD as solubilizer. The mixture was boiled under reflux for several hours. Subsequent cooling yielded a mixture of deuterated and undeuterated indazole, which was dried under vacuum for at least 24 h.

The molecules in the supersonic jet were excited by the unfocused beam of a frequency-doubled pulsed dye laser (Spectra Physics PDL 3) pumped by a Nd : YAG laser (Continuum Powerlite 8020) at 20 Hz repetition rate. The dye laser beam was profiled to 5 mm diameter circular shape using a telescope and two apertures. The distance from the nozzle orifice to the laser beam was typically 5 mm. LIF excitation spectra were taken by collecting and focusing the fluorescence with an $f = 50$ mm lens at right angles onto a photomultiplier tube (Hamamatsu R928) connected to a boxcar integrator (Stanford Research SR250) and a PC desktop computer running a LabView program. For DF spectra, the fluorescence was focused onto the entrance slit of a 750 mm spectrograph (Jobin-Yvon Spex 750M) with a 1200 lines/mm grating. The dispersed spectra were detected using an image-intensified CCD camera (Princeton Instruments ICCD-576-G/1, 576×384 pixels). Scattered laser light was subtracted afterwards by taking a background spectrum with the molecular beam valve off. The experimental spectral resolution was essentially limited by the CCD camera (± 1 pixel). Including possible calibration errors, the uncertainties in the measured vibrational peak positions in the DF spectra are about $\pm 3\,\mathrm{cm}^{-1}$.

Mass spectra were measured using resonant two-photon ionization (R2PI) in a linear time-of-flight spectrometer. The laser source was a second frequency-doubled Nd : YAG-pumped dye laser (Lambda Physics FL3002 & Innolas Spitlight 1200). A seeded molecular beam of indazole expanded into the high vacuum chamber of the mass spectrometer through a 0.5 mm wide skimmer about 1 cm downstream from the heated pulsed valve source. The molecular beam and the focused dye laser beam crossed between the repeller and extractor plates of a Wiley-McLaren electrode assembly. The resulting ions were separated according to their flight times in a 1 m field-free drift zone and detected by a microchannel plate (Hamamatsu F4294-07) connected to a 350 MHz, 1 GSample/s digital oscilloscope (LeCroy LT264). The mass spectra were obtained at a fixed laser wavelength by averaging over 2000 laser shots.

Ground state geometry optimizations for the Ia-*h* and Ia-*d* monomers were performed by density functional theory (DFT) calculations using the TPSS functional of Tao, Perdew, Staroverov and Scuseria [23,24] and the aug-cc-pVTZ basis set as implemented in the GAUSSIAN03 program suite [25]. The state-of-the-art TPSS functional has been reported to predict harmonic vibrational frequencies with an rms error $< 20\,\mathrm{cm}^{-1}$ without need for empirical scaling factors [24], which eliminates a major source of ambiguity from such calculations. The normal mode vibrations for Ia-*h* and Ia-*d* were computed at the minimum-energy structures without symmetry restrictions.

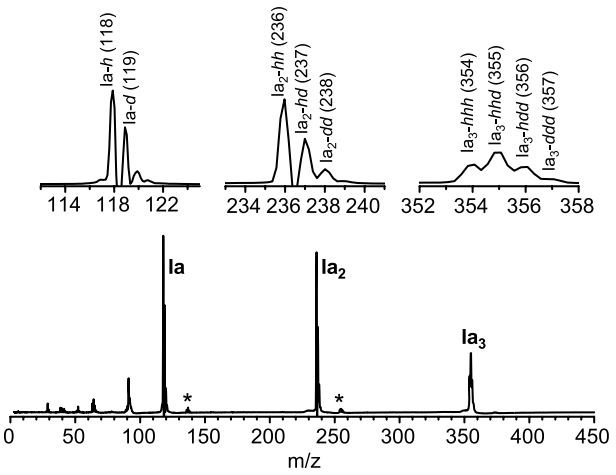

Fig. 2. R2PI mass spectrum of the mixture of plain and deuterated indazole. The traces above the main peaks show expanded views for the Ia monomers, dimers, and trimers. $\nu_{\text{excitation}} = 34\,147.4\ \text{cm}^{-1}$.

3. Results and discussion

3.1 R2PI mass spectra

Figure 2 shows an R2PI mass spectrum for the mixed Ia-*h*/Ia-*d* sample. The prominent peaks at $m = 118$ and 119 Dalton confirm the presence of the Ia-*h* and Ia-*d* monomers in the molecular beam. Signals at lower masses arise by fragmentation of the molecules during the ionization, peaks at twice and three times the monomer masses are assigned to H-bonded indazole dimers and trimers. The dimer isotopologues appear as a triplet of mass peaks at 236, 237 and 238 Dalton, and the trimer isotopologues as a partially resolved quadruplet at 354–357 Dalton. The weak signals marked with an asterisk are shifted from the monomer and dimer peaks by 18 mass units and assigned to corresponding complexes with water. Our previous study revealed that indazole–water complexes are easily formed, when the sample contains just a trace amount of water [10,14]. Only the two monomers Ia-*h* and Ia-*d* will be of interest to us in this paper in the following.

3.2 LIF excitation spectra

LIF excitation scans of Ia-*h* and the Ia-*h*/Ia-*d* mixture in the region around the electronic origin band of Ia-*h* are depicted in Fig. 3. The strong peak at $\nu_0(\text{Ia}-h) = 34\,471.69\ \text{cm}^{-1}$ (Fig. 3a) has previously been identified from rotationally resolved $S_1 \leftarrow S_0$ LIF excitation spectra measured in a molecular beam as the electronic origin band (0_0^0 transition) of Ia-*h* [9,10]. The excitation spectrum of the Ia-*h*/Ia-*d* mixture in Fig. 3b shows a second, similarly strong band at $34\,479.5 \pm 1.0\ \text{cm}^{-1}$, *i.e.*, $7.8\ \text{cm}^{-1}$ above the Ia-*h* 0_0^0 transition. That peak is therefore assigned to the electronic origin (0_0^0 transition) of Ia-*d*, $\nu_0(\text{Ia-}d) = 34\,479.5\ \text{cm}^{-1}$. The assignment agrees with Yang and Tzeng [26], although the blue-shift they reported is a little smaller ($5\ \text{cm}^{-1}$).

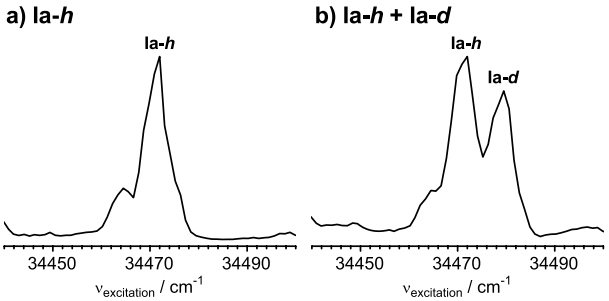

Fig. 3. LIF excitation scans around the $S_1 \leftarrow S_0$ origin bands of **(a)** plain indazole and **(b)** the mixture of plain and deuterated indazole.

A shift by $\Delta\nu_0(\text{Ia-}d - \text{Ia-}h) = 7.8\,\text{cm}^{-1}$ in the $S_1 - S_0$ transition frequency on deuteration is nothing unusual. It can be explained by a slight decrease in zero-point level energy (ZPL) resulting from slightly different normal mode frequencies in both S_0 and S_1 states (see, *e.g.*, [27,28]). If the lowering of ZPL in the S_1 state is larger than in the S_0 state, the $S_1 - S_0$ origin band is red-shifted, in the opposite case it is blue-shifted. Depending on the deuteration site, either a blue-shift or a red-shift can occur. If the deuteration does not cause a large change in molecular structure, the origin band shift is typically below $\approx 10\,\text{cm}^{-1}$ [27,28]. This seems to be the case here, where the decrease in S_1 ZPL is just $7.8\,\text{cm}^{-1}$ smaller than in S_0. The observed isotope effect is an important tool to distinguish the isotopologues and hence the structure of the indazole complexes [13].

3.3 DF spectra

DF spectra of Ia-*h* and Ia-*d* after excitation of the molecules *via* their $S_1 \leftarrow S_0$ origin bands are displayed in Fig. 4. Comparison of the two spectra reveals that their lower energy parts, up to $800\,\text{cm}^{-1}$ from the excitation frequency (ν_0), look rather similar. Two prominent bands in that region located at $\nu_0 - \nu_{\text{fl}} \approx 612$ and $\approx 764\,\text{cm}^{-1}$ exist for both Ia-*h* and Ia-*d*. At higher vibrational energies, the spectrum of Ia-*d* begins to differ from that of Ia-*h*. For instance, a very strong band appears for Ia-*h* at $\nu_0 - \nu_{\text{fl}} = 1077\,\text{cm}^{-1}$, whereas Ia-*d* shows two moderately strong bands at $\nu_0 - \nu_{\text{fl}} = 1007$ and $1119\,\text{cm}^{-1}$.

3.4 Computational results

The nature of the S_0 vibrations of Ia-*h* and Ia-*d* seen in the DF spectra was explored by TPSS/aug-cc-pVTZ frequency calculations. As a planar 15-atom molecule with C_s symmetry, Ia has 39 normal mode vibrations which are grouped into 27 in-plane (a') and 12 out-of-plane (a'') modes. The calculated nuclear displacement vectors for Ia-*h* and Ia-*d* are displayed in Fig. 5, the obtained harmonic vibrational frequencies are compiled in Table 1.

The calculated TPSS/aug-cc-pVTZ in-plane modes for Ia-*h* turned out similar to those from our earlier less accurate MP2/6-31G calculation [10]. However, three of the previous in-plane modes ($\nu_{10} - \nu_{12}$) were renumbered: The old ν_{11} matches better with

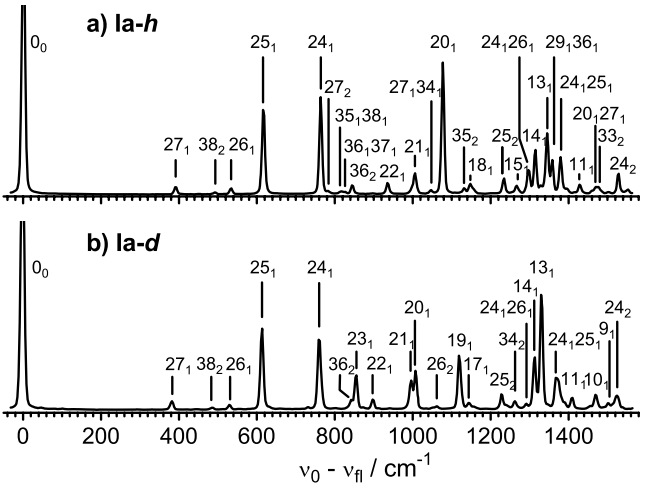

Fig. 4. DF spectra of Ia-*h* and Ia-*d* from their $S_1 - S_0$ origin bands ($\nu_0 = 34\,471.7$ and $34\,479.5\,\mathrm{cm}^{-1}$, respectively).

the new ν_{10}, the old ν_{12} corresponds to the new ν_{11}, and the old ν_{10} to the new ν_{12} judged by the mode shapes. The TPSS/aug-cc-pVTZ out-of-plane modes $\nu_{31} - \nu_{37}$ show larger deviations from the earlier MP2/6-31G results. The former $\nu_{29} - \nu_{34}$ are more similar to the current $\nu_{30} - \nu_{35}$, while the former ν_{31} and ν_{35} do not seem to have direct equivalents among the TPSS/aug-cc-pVTZ modes. The similarity in mode shape seems to correlate with the closeness in the calculated vibrational frequency.

The effect of deuteration is immediately seen by inspecting the respective normal modes of Ia-*h* and Ia-*d* in Fig. 5. Table 1 presents our preferred correlation between the two isotopologues judged by comparison of the frequencies and nuclear displacement vectors, although alternatives may exist in some cases. Most modes have a direct counterpart in the other isotopologue with almost the same frequency (*cf.* Table 1) and almost the same mode shape (*cf.* Figs. 5a and 5b). If this is the case we can speak practically about the same vibration for both isotopologues. As expected, the difference in frequency is more pronounced for modes with significant shares of NH/ND motion. Thus, the isotope effect is the largest for the NH/ND stretching (ν_1 for Ia-*h*, ν_6 for Ia-*d*), in-plane bending (ν_{15} for Ia-*h*, ν_{23} for Ia-*d*), and out-of-plane bending (ν_{37}) modes. The differences between the vibrations of Ia-*h* and Ia-*d* are reflected by corresponding variations in the band frequencies and intensities in the DF spectra in Figs. 4a and 4b.

3.5 Vibrational assignments

Considering the nature of the $S_1(A') \leftrightarrow S_0(A')$ electronic transition of indazole with its transition dipole moment in the plane of the molecule, the DF spectrum from the S_1 origin is expected to show the in-plane (a') vibrations in the S_0 state by electric-dipole allowed transitions to the respective fundamentals and to possible overtone or combination states. Transitions from the S_1 origin to the S_0 out-of-plane (a'') fundamentals are

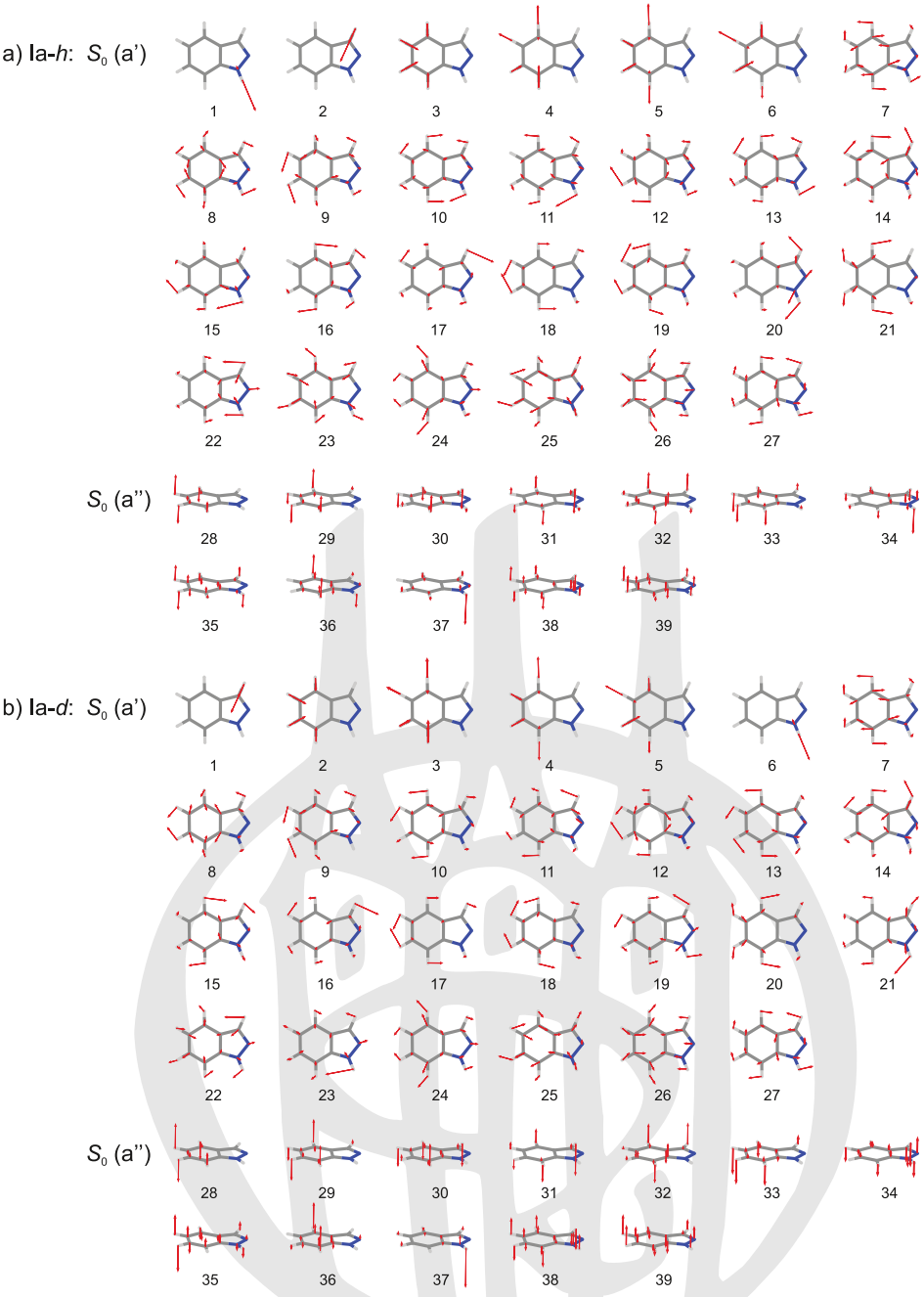

Fig. 5. Calculated normal mode vibrations for **(a)** Ia-*h* and **(b)** Ia-*d* in the electronic ground state at the TPSS/aug-cc-pVTZ level of theory.

Table 1. Observed and calculated S_0 state vibrational frequencies for Ia-*h* and Ia-*d*. Corresponding vibrations of Ia-*h* and Ia-*d* are listed in the same row for comparison.

	Ia-*h*						Ia-*d*			
sym.	mode	observed DF		calculated[a]		observed IR[b]	mode	observed DF		calculated[a]
		ν/cm^{-1}	intens.	ν/cm^{-1}	IR intens.	ν/cm^{-1}		ν/cm^{-1}	intens.	ν/cm^{-1}
a'	1			3607	74.	3524 s	6			2649
	2			3199	4.9	3120 w	1			3199
	3			3155	15.	3080 m	2			3156
	4			3147	28.	3067 m	3			3147
	5			3137	4.5	3059 m	4			3137
	6			3128	0.0	3047[c] w	5			3128
	7			1624	12.	1626 m	7			1621
	8			1588	0.6	1586[d] w	8			1582
	9	1502[e]	vw	1507	7.7	1503 m	9	1503[e]	vw	1506
	10	1476[f]	w	1491	4.8	1481[f] w	10	1469[f]	w	1477
	11	1428	w	1429	4.5	1429 w	11[g]	1410	w	1407
	12	1358	m	1395	3.4	1360 m	12			1389
	13	1345	s	1367	23.	1347 m	13[g]	1330	vs	1332
	14	1315	s	1314	5.2	1316 vw	14	1314	s	1311
	15	1267	w	1265	1.8	1267 w				
	16	1245[h]		1248	6.7	1244 w	15			1247
	17	1205[h]		1210	4.6	1203 w	16			1214
	18	1148[i]	w	1157	3.9	1149 w	17	1143	w	1158
	19	1125[h]		1129	3.2	1124 w	18			1129
	20	1077	vs	1067	14.	1078 w	19[g]	1119	s	1120
	21	1006	m	1013	8.4	1007 w	20	1007	m	1015
	22	935	m	928	33.	937 s	21[g]	996	m	990
	23	900[h]		891	2.0	903 w	22	897	w	896
							23	856	m	852
	24	764	vs	765	5.7	765 w	24	759	vs	763
	25	616	vs	613	1.6	618 vw	25	614	vs	611
	26	535	w	532	0.3		26	529	w	530
	27	391	w	392	1.1	397 vw	27	382	w	384
a''	28			974	0.0		28			974
	29			938	1.5		29			938
	30			853	12.	850 s	30			852
	31			837	20.	832 s	31			836
	32			755	3.8		32			755
	33	741[h]		746	45.	739 vs	33			745
	34	657		655	45.	652 s	34	631		632
	35	566		572	3.1	565 vw	35			565
	36	422		426	0.0		36[g]	421		424
	37	406[h]		414	51.	405 s	37	310		323
	38	246		245	0.2		38	243		242
	39	205[h]		207	1.5		39			205

[a] Unscaled harmonic vibrational wavenumbers from TPSS/aug-cc-pVTZ calculation.
[b] From Cané *et al.* [8].
[c] An alternative would be the observed IR band at 3033 cm^{-1}.
[d] Another possible assignment instead of 8_1 is 33_130_1.
[e] Another possible assignment instead of 9_1 is 32_2.
[f] Another possible assignment instead of 10_1 is 33_2.
[g] Vibration has somewhat different shape than for Ia-*h*.
[h] From the analysis of DF spectra from S_1 excited vibronic states [10].
[i] Overlapped with the 25_126_1 band.

Table 2. Observed and calculated wavenumbers of some S_0 state combination and overtone vibrations for Ia-*h* and Ia-*d* in the measured DF spectra. Corresponding vibrations of Ia-*h* and Ia-*d* are shown in the same row for comparison.

Ia-*h*				Ia-*d*			
observed DF		assignment	calculated[a]	observed DF		assignment	calculated[a]
ν/cm^{-1}	intens.		ν/cm^{-1}	ν/cm^{-1}	intens.		ν/cm^{-1}
492	vw	38_2	490	487	vw	38_2	485
783	w	27_2	784				
814	vw	35_138_1	817				
827	vw	36_137_1	840	731	vw	36_137_1	747
844	w	36_2	852	842	w	36_2	849
1047	w	27_134_1	1047				
				1062	vw	26_2	1060
1132	w	35_2	1144				
1235	w	25_2	1226	1227	w	25_2	1222
				1262	w	34_2	1264
1297	m	24_126_1	1297	1292	vw	24_126_1	1293
1358	m	29_136_1	1364				
1380	m	24_125_1	1378	1370	m	24_125_1	1374
1470	w	20_127_1	1459				
1529	m	24_2	1530	1525	w	24_2	1525

[a] From TPSS/aug-cc-pVTZ calculation.

electric dipole-forbidden, out-of-plane vibrations are therefore expected only through transitions to two-quantum overtone or combination states.

The assigned fundamentals in the DF spectra of both Ia isotopologues are given in Table 1 together with the calculated TPSS/aug-cc-pVTZ frequencies. The main criterium for finding and confirming their assignment was the proximity of the observed and predicted wavenumbers. The frequencies and intensities from the IR absorption data for Ia-*h* of Cané *et al.* [8] provided additional support and have been included in Table 1 together with our calculated IR intensities. The out-of-plane fundamentals in Table 1 were deduced from the observed overtone and combination frequencies. A list of the assigned overtone and combination states with discernible DF band intensities is found in Table 2.

A vibrational analysis of the S_0 state of Ia-*h* had already been undertaken in our first publication [10] based on the DF spectra from several S_1 vibronic states, the vibrational frequencies from an MP2/6-31G calculation and the IR data of Cané *et al.* [8]. The more accurate present TPSS/aug-cc-pVTZ results confirmed the previous assignments for the in-plane modes of Ia-*h*, but required a reassignment of the out-of-plane modes. First, modes $\nu_{29} - \nu_{35}$ of the previous work now correspond to modes $\nu_{30} - \nu_{36}$ in this work. Furthermore, three out-of-plane fundamentals had been listed in the previous work in the 400 cm^{-1} region, at 406, 415 and 424 cm^{-1}. However, the TPSS/aug-cc-pVTZ method predicted the existence of only two vibrations in that range, ν_{37}(Ia-*h*) = 414 cm^{-1} and ν_{36}(Ia-*h*) = 426 cm^{-1} (*cf.* Table 1). The DF spectra confirmed the existence of those fundamentals at 406 and 422 cm^{-1} (424 cm^{-1} in the previous work) by the appearance of combinations involving those vibrations after

excitation of five different S_1 vibronic states [10], but the experimental evidence for a 415 cm^{-1} mode apart from the report in the IR spectrum [8] had been scarce and less reliable [10]. The measured fundamentals at $\nu = 406$ and 422 cm^{-1} are therefore now unambiguously assigned to ν_{37}(Ia-*h*) and ν_{36}(Ia-*h*), respectively. The necessary assertion that a 415 cm^{-1} out-of-plane fundamental does not exist for Ia-*h* thus leads to excellent agreement between all observed and calculated frequencies and agreement between the observed and the calculated IR intensities (Table 1).

The assignment of the vibrational bands in the DF spectrum of Ia-*d* was mostly guided by comparison with the TPSS/aug-cc-pVTZ vibrational frequencies. The correlation of the band intensities and frequencies with those in the DF spectrum of Ia-*h* provided further support. As neither IR absorption data nor DF data from S_1 excited vibronic states are available, the number of assigned vibrations for Ia-*d* is lower than in the Ia-*h* case. The DF spectrum of Ia-*h* was found to be dominated by three intense bands, which were assigned to ν_{25}(Ia-*h*) = 616 cm^{-1}, ν_{24}(Ia-*h*) = 764 cm^{-1}, and ν_{20}(Ia-*h*) = 1077 cm^{-1}. With red-shifts of just 2 resp. 5 cm^{-1}, the first two modes (ν_{25}(Ia-*d*) = 614 cm^{-1}, ν_{24}(Ia-*d*) = 759 cm^{-1}) also appear prominently in the DF spectrum of Ia-*d*.

Larger discrepancies can be noticed only at $\nu > 800$ cm^{-1}. In particular, the strong intensity of the band of ν_{20}(Ia-*h*) = 1077 cm^{-1} in the Ia-*h* DF spectrum appears to be shared by two moderately intense bands in the Ia-*d* DF spectrum, one red-shifted by 70 cm^{-1} and the other blue-shifted by 42 cm^{-1} compared to ν_{20}(Ia-*h*). The corresponding Ia-*d* vibrations are assigned as ν_{20}(Ia-*d*) = 1007 cm^{-1} and ν_{19}(Ia-*d*) = 1119 cm^{-1}. The comparision of Figs. 5a and 5b shows that ν_{20}(Ia-*h*) indeed has no exact Ia-*d* counterpart, although some similarity with mode ν_{19}(Ia-*d*) is recognizable. The involvement of significant NH/ND motion in both modes explains why the similarity is only partial. Analogously, ν_{21}(Ia-*d*) has a similar frequency as ν_{22}(Ia-*h*). However, as can also be seen from Figs. 5a and 5b, ν_{21}(Ia-*d*) exhibits sizable ND bending motion, which makes it clearly different from ν_{22}(Ia-*h*). An additional remarkable feature in the Ia-*d* spectrum is the high intensity of the band assigned to ν_{13}(Ia-*d*) = 1330 cm^{-1}.

Apart from a few exceptions, the observed and calculated vibrational frequencies for Ia-*h* and Ia-*d* in Table 1 match within 1%. The exceptions are the high-frequency modes $\nu_1 - \nu_6$ of Ia-*h* with observed-to-calculated ratios of about 0.975, ν_{12}(Ia-*h*) and ν_{13}(Ia-*h*) with ratios of 0.97 and 0.98, and the ν_{37} mode with ratios of 0.98 (Ia-*h*) and 0.96 (Ia-*d*). While a theoretical treatment of the vibrational anharmonicities was beyond the scope of this study, the differences in the case of the high-frequency modes ($\nu_1 - \nu_6$) and for ν_{12} and ν_{13} likely have to be attributed to their effect. Anharmonic calculations would be feasible for the Ia monomers, but are still prohibitively expensive for the H-bonded Ia dimers, where they would require several months of CPU time with the resources available to us. Moreover, the corrections for the low frequency vibrations of smaller rigid aromatic molecules are typically very small, often < 1–3 cm^{-1} for $\Delta v = +1$ transitions [28] and therefore below our experimental resolution. For some bending modes, it may even happen that the anharmonicities are slightly negative. In that case, the two-quantum overtone or combination states should be slightly higher in energy than twice the fundamental energy. This appears to be observed for some assigned overtone and combination states in Table 2, but such shifts remain again below a few cm^{-1}. Mode ν_{37}, eventually, is a special case. ν_{37} is the N–H/N–D out-of-plane

bending vibration of Ia-*h*/Ia-*d* which is of very low frequency in both isotopologues (406 resp. 310 cm^{-1}), indicating a very shallow, almost flat potential energy minimum around the planar geometry. This is likely to require a much higher level of theory for a reliable prediction of the potential energy function. Problems of that type are also encountered, for example, in the case of NH and NH_2 out-of-plane vibrations of nucleic acid bases (see, *e.g.*, [29]).

4. Conclusions

Dispersed fluorescence (DF) spectra of 1H- and 1D-indazole have been measured in the present work in a seeded supersonic free jet in He following excitation of the $S_1 \leftarrow S_0$ origin bands of the molecules at ν_0(Ia-*h*) = 34 471.7 cm^{-1} and ν_0(Ia-*d*) = 34 479.5 cm^{-1}, respectively. The shift in the $S_1 \leftrightarrow S_0$ transition frequency on deuteration can be explained by a slightly smaller decrease in zero-point energy in the S_1 compared to the S_0 state. The measurements were accompanied by ground state structure optimizations and vibrational frequency calculations using DFT at the TPSS/aug-cc-pVTZ level. Vibrational assignments for both isotopologues in their electronic ground states were developed based on comparisons of the observed frequencies and relative band intensities for Ia-*h* and Ia-*d* and by comparison with the respective calculated frequencies.

Information on the electronic spectrum of Ia-*d* in the gas phase has previously been limited to the recent R2PI spectra of Yang and Tzeng [26], who assigned a number of vibronic transitions in the $S_1 \leftarrow S_0$ excitation spectrum based on the accordance with Ia-*h* and with CIS/6-311++G** frequency calculations. Our value for the Ia-*d* origin agrees with that reported by Tzeng and Yang (34 478 cm^{-1}), but should be slightly more accurate. Fluorescence measurements for Ia-*d* have not yet been available to the best of our knowledge.

The dispersed fluorescence spectra for Ia-*h* and Ia-*d* from their S_1 origins obtained in the present work comprise transitions to the in-plane fundamentals and to much weaker overtone and two-quantum combination states of the out-of-plane vibrations. The observed and calculated S_0 frequencies match within 1–3%. Significant differences were observed practically only for vibrations involving motion of the NH/ND group.

In a forthcoming publication [13], we will focus on the excitation and dispersed fluorescence spectra of the H-bridged homodimers and mixed dimers of Ia-*h* and Ia-*d*, which are of considerable interest as model systems for double proton transfer in H-bonded complexes. The data about the two isotopomeric monomers gathered in the present work give the necessary requirements to unravel and interpret the dimer spectra. It will be seen that many of the monomer vibrations appear in the dimer spectra as well. In addition, we will give a full account of the low-frequency intermolecular vibrations in the dimers in the S_1 and S_0 states.

In the first place, however, the analysis of the vibronic bands in the homodimers and in the mixed dimer of Ia-*h* and Ia-*d* will allow us to determine the size of the elusive exciton splitting between the excited electronic states shared by both Ia moieties in the dimer [13]. Owing to the two possible relative orientations of the transition dipole moments of the two monomer units in the dimer, the dimer has two nearly isoener-

getic excited electronic states, S_1 and S_2, which are split by dipole–dipole coupling as described by Frenkel exciton theory [30]. The two excited-state wave functions of the dimer formed from two equivalent moieties ϕ_A and ϕ_B, where either one can be excited (ϕ_A^* or ϕ_B^*), are given by the linear combinations $\psi_\pm^* = 2^{-1/2}(\phi_A^*\phi_B \pm \phi_A\phi_B^*)$. For the planar, C_{2h} symmetric homodimers Ia_2-*hh* and Ia_2-*dd*, however, only the $S_2(B_u) \leftarrow S_0(A_g)$ electronic transition to the energetically higher component of the exciton doublet is symmetry allowed considering the b_u symmetric transition dipole of the dimers. The $S_1(A_g) \leftarrow S_0(A_g)$ electronic transition to the lower component of the exciton doublet has zero oscillator strength because of the anti-parallel combination of the two monomer transition dipoles and is strictly forbidden. For the mixed dimer Ia_2-*hd*, however, the C_{2h} symmetry is broken and both S_1 and S_2 electronic origins are experimentally observed [13]. An $S_2 - S_1$ distance of $\Delta E_{hd} = 23$ cm^{-1} was measured. Furthermore, it turns out that the lower (S_1) exciton component is observable in the homodimers in combination with excited b_u symmetric vibrations of the dimer, while such b_u vibrations cannot be observed in the higher (S_2) state. A detailed vibrational analysis of the electronic spectra of the dimers, which is in progress [13] building on the foundations layed in the present paper, will paint a fairly comprehensive picture of the exciton coupling in the dimer.

Acknowledgement

This work has been supported by the Fonds der Chemischen Industrie and the Deutscher Akademischer Austauschdienst (DAAD). E. J. acknowledges support from the Estonian Science Foundation (Grant no. 8674).

References

1. J. Catalán, J. C. del Valle, R. M. Claramunt, G. Boyer, J. Laynez, J. Gómez, P. Jiménez, F. Tomás, and J. Elguero, J. Phys. Chem. **98** (1994) 10606.
2. J. Catalán, J. L. G. de Paz, and J. Elguero, J. Chem. Soc., Perkin Trans. **2** (1996) 57.
3. H.-U. Schütt and H. Zimmermann, Ber. Bunsenges. Phys. Chem. **67** (1963) 54.
4. J. P. Byrne and I. G. Ross, Aust. J. Chem. **24** (1971) 1107.
5. B. Velino, E. Cané, A. Trombetti, G. Corbelli, F. Zerbetto, and W. Caminati, J. Mol. Spectrosc. **155** (1992) 307.
6. A. Bigotto and C. Zerbo, Spectrosc. Lett. **23** (1990) 65.
7. E. Cané, A. Trombetti, B. Velino, and W. Caminati, J. Mol. Spectrosc. **155** (1992) 307.
8. E. Cané, P. Palmieri, and A. Trombetti, J. Chem. Soc. Faraday Trans. **89** (1993) 4005.
9. G. Berden, W. L. Meerts, and E. Jalviste, J. Chem. Phys. **103** (1995) 9596.
10. E. Jalviste and F. Temps, J. Chem. Phys. **111** (1999) 3898.
11. H. Su, M. Pradhan, and W. B. Tzeng, Chem. Phys. Lett. **411** (2005) 86.
12. J. Oomens, G. Meijer, and G. von Helden, Int. J. Mass Spectrom. **249–250** (2006) 199.
13. H. Nicken, F. Temps, and E. Jalviste, to be published.
14. E. Jalviste, S. Dziarzhytski, and F. Temps, Z. Phys. Chem. **222** (2008) 695.
15. J. L. G. de Paz, J. Elguero, C. Foces-Foces, A. L. Llamas-Saiz, F. Aguilar-Parilla, O. Klein, and H. H. Limbach, J. Chem. Soc., Perkin Trans. **2** (1997) 101.
16. O. Klein, F. Aguilar-Parrilla, J. M. Lopez, N. Jagerovic, J. Elguero, and H. H. Limbach, J. Am. Chem. Soc. **126** (2004) 11718.
17. J. P. Castaneda, G. S. Denisov, S. Y. Kucherov, V. M. Schreiber, and A. V. Shurukhina, J. Mol. Struct. **660** (2003) 25.
18. C. A. Rice, N. Borho, and M. A. Suhm, Z. Phys. Chem. **219** (2005) 379.

19. T. N. Wassermann, C. A. Rice, M. A. Suhm, and D. Luckhaus, J. Chem. Phys. **127** (2007) 234309.
20. V. Poterya, O. Tkáč, J. Fedor, M. Fárník, P. Slaviček, and U. Buck, Int. J. Mass Spectrom. **290** (2010) 85.
21. I. C. Walker, M. H. Palmer, M. J. Hubin-Franskin, and J. Delwiche, Chem. Phys. Lett. **367** (2003) 517.
22. G. A. King, T. A. A. Oliver, M. G. D. Nix, and M. N. R. Ashfold, J. Chem. Phys. **132** (2010) 064305.
23. J. M. Tao, J. P. Perdew, V. N. Staroverov, and G. E. Scuseria, Phys. Rev. Lett. **91** (2003) 146401.
24. V. N. Staroverov, G. E. Scuseria, J. Tao, and J. P. Perdew, J. Chem. Phys. **119** (2003) 12129.
25. M. J. Frisch, G. W. Trucks, H. B. Schlegel, G. E. Scuseria, M. A. Robb, J. R. Cheeseman, J. A. Montgomery Jr., T. Vreven, K. N. Kudin, J. C. Burant, J. M. Millam, S. S. Iyengar, J. Tomasi, V. Barone, B. Mennucci, M. Cossi, G. Scalmani, N. Rega, G. A. Petersson, H. Nakatsuji, M. Hada, M. Ehara, K. Toyota, R. Fukuda, J. Hasegawa, M. Ishida, T. Nakajima, Y. Honda, O. Kitao, H. Nakai, M. Klene, X. Li, J. E. Knox, H. P. Hratchian, J. B. Cross, C. Adamo, J. Jaramillo, R. Gomperts, R. E. Stratmann, O. Yazyev, A. J. Austin, R. Cammi, C. Pomelli, J. W. Ochterski, P. Y. Ayala, K. Morokuma, G. A. Voth, P. Salvador, J. J. Dannenberg, V. G. Zakrzewski, S. Dapprich, A. D. Daniels, M. C. Strain, O. Farkas, D. K. Malick, A. D. Rabuck, K. Raghavachari, J. B. Foresman, J. V. Ortiz, Q. Cui, A. G. Baboul, S. Clifford, J. Cioslowski, B. B. Stefanov, G. Liu, A. Liashenko, P. Piskorz, I. Komaromi, R. L. Martin, D. J. Fox, T. Keith, M. A. Al-Laham, C. Y. Peng, A. Nanayakkara, M. Challacombe, P. M. W. Gill, B. Johnson, W. Chen, M. W. Wong, C. Gonzalez, and J. A. Pople, Gaussian 03, Revision C.02, Gaussian, Inc., Wallingford CT (2004).
26. S. C. Yang and W. B. Tzeng, Chem. Phys. Lett. **501** (2010) 6.
27. J. Lin, J. L. Lin, and W. B. Tzeng, Chem. Phys. **295** (2003) 97.
28. P. Kolek, S. Léscniewski, M. Andrzejak, M. Góra, P. Cias, A. Węgrzynowicz, and J. Najbar, J. Mol. Spectrosc. **264** (2010) 129.
29. W. Zierkiewicz, L. Komorowski, D. Michalska, J. Cerny, and P. Hobza, J. Phys. Chem. B **112** (2008) 16734.
30. A. S. Davydov, *Theory of Molecular Excitons*. McGraw-Hill, New York (1962).